

**$\phi$  meson mass and decay width in nuclear matter**

D. Cabrera\*

*Departamento de Física Teórica and IFIC, Centro Mixto Universidad de Valencia-CSIC, Institutos de Investigación de Paterna, Apartado Correos 22085, E-46071 Valencia, Spain*M. J. Vicente Vacas<sup>†</sup>*Departamento de Física Teórica and IFIC, Centro Mixto Universidad de Valencia-CSIC, Institutos de Investigación de Paterna, Apartado Correos 22085, E-46071 Valencia, Spain*

(Received 4 June 2002; published 29 April 2003)

The  $\phi$  meson spectrum, which in vacuum is dominated by its coupling to the  $\bar{K}K$  system, is modified in nuclear matter. Following a model based on chiral SU(3) dynamics we calculate the  $\phi$  meson self-energy in nuclear matter considering the  $K$  and  $\bar{K}$  in-medium properties. For the latter we use the results of previous calculations which account for  $S$ - and  $P$ -wave kaon-nucleon interactions based on the lowest order meson-baryon chiral effective Lagrangian, and this leads to a dressing of the kaon propagators in the medium. In addition, a set of vertex corrections is evaluated to fulfill gauge invariance, which involves contact couplings of the  $\phi$  meson to  $S$ -wave and  $P$ -wave kaon-baryon vertices. Within this scheme the mass shift and decay width of the  $\phi$  meson in nuclear matter are studied.

DOI: 10.1103/PhysRevC.67.045203

PACS number(s): 13.25.-k, 14.40.Cs, 25.80.-e

**I. INTRODUCTION**

The study of the renormalization of the hadron properties (such as effective masses and widths) in a hot/dense baryonic medium has been a matter of wide interest during the last years (see, for instance, Ref. [1]). Electromagnetic decays of vector mesons are specially suited to explore the high densities that occur in nuclei or neutron stars, since the emitted dilepton pairs, which carry the spectral information of the vector meson in the moment of the decay, undergo a low distortion before they abandon the dense medium and reach the detector. In particular, the  $\phi$  meson stands as a unique probe for a possible partial restoration of chiral symmetry in hadronic matter, since it does not overlap with other light resonances in the mass spectrum. In addition, the modification of the  $\phi$  properties in the medium is strongly related to the renormalization of the kaon properties in the medium, a topic that has also received much attention because of notable deviations from the low density theorem needed to reproduce kaonic atoms data [2–5] and the possibility of formation of kaon condensates in neutron stars [6]. The  $\phi$  properties in a nuclear medium could be tested through detection of its decay products in  $A$ - $A$  and  $p$ - $A$  collisions [7], by means of the reaction  $\pi^- p \rightarrow \phi n$  in nuclei [8] or the recently proposed method based on inclusive  $\phi$  photoproduction in nuclei [9].

Concerning the change of the  $\phi$  properties in the medium, much of the work done has been partly stimulated by the idea that partial restoration of chiral symmetry may modify the masses of mesons at finite temperature and/or density. The  $\phi$  mass change has been studied in several approaches such as using effective Lagrangians [8,10–13], QCD sum

rules [14,15], or the Nambu–Jona-Lasinio model [16]. The  $\phi$  width modification in matter has also been a subject of study in a dropping meson mass scenario [12,17–21], as a result of collisional broadening through  $\phi$ -baryon [22] or  $\phi$ -meson [23] scattering processes and on the basis of modifications of the main decay channels in vacuum [8,24]. All these works point at a sizable renormalization of the  $\phi$  width and a small mass shift.<sup>1</sup>

The purpose of this work is to obtain the  $\phi$ -meson self-energy in cold, symmetric nuclear matter from which we shall study how the mass and decay width are modified in the medium. We follow the lines of Ref. [24] in which the main input to the calculation of the  $\phi$  self-energy in nuclear matter is the kaon self-energy of Ref. [25], arising from  $S$ - and  $P$ -wave interactions with the nucleons. The  $S$ -wave kaon self-energy is obtained from a self-consistent coupled channel unitary calculation of the  $\bar{K}N$  amplitude based on effective chiral Lagrangians, in which Pauli blocking, the renormalization of the pions, and mean-field potentials of the baryons in the intermediate states are taken into account. The  $P$ -wave kaon self-energy is driven by the coupling to hyperon-hole excitations. Although we adhere to this approach for the kaon self-energy, we introduce some technical novelties. Whereas the work in Ref. [24] is devoted to the calculation of the in-medium  $\phi$  width and thus only the imaginary part of the  $\phi$  self-energy is obtained, we also focus on the real part to look for the shift in the  $\phi$  mass. This leads us to improve the model of Ref. [24] by including additional mechanisms required by gauge invariance as well as performing a finer study of the relativistic recoil corrections considered in the  $P$ -wave kaon self-energy. In Sec. II we detail our model of the  $\phi$  self-energy for which we ad-

\*Email address: Daniel.Cabrera@ific.uv.es

<sup>†</sup>Email address: Manuel.J.Vicente@ific.uv.es<sup>1</sup>Except for Ref. [14], in which a mass shift of a few hundred MeV is reported under hot and dense matter conditions.

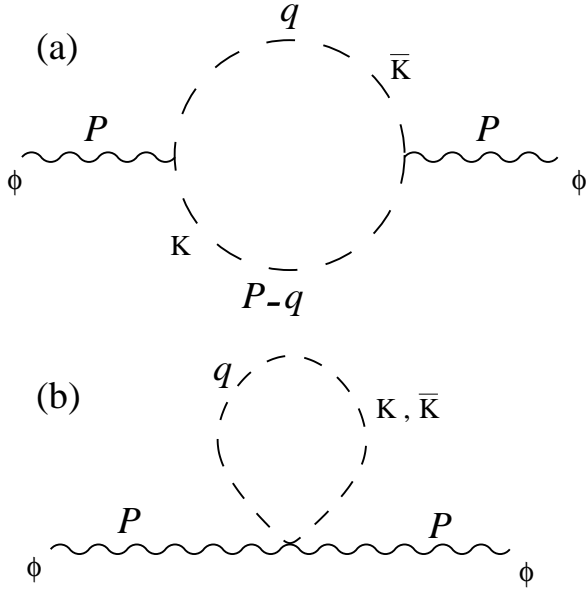


FIG. 1. Diagrams contributing to the  $\mathcal{O}(g_\phi^2)$   $\phi$  self-energy in free space: (a) two-kaon loop, (b) kaon tadpole.

here to the vector field representation of Ref. [8].  $S$ - and  $P$ -wave kaon self-energies are quoted as the major input of the calculation in nuclear matter and a set of vertex corrections involving contact,  $\phi$ -meson-baryon vertices, are considered as requested by gauge invariance. In Sec. III we present our results for the  $\phi$  self-energy and the consequent findings for the  $\phi$  mass shift and width, and summarize our conclusions.

## II. $\phi$ -MESON SELF-ENERGY IN VACUUM AND IN NUCLEAR MATTER

In this work we shall deal with the coupling of the  $\phi$  to  $K\bar{K}$  channels, which in vacuum accounts for 85% of the total decay width. It was found in Refs. [8,24] that the in-medium  $\bar{K}K$  related channels give rise to a  $\phi$  width several times larger than in free space. Here we shall focus on the in-medium modifications of the whole  $\phi$ -meson self-energy (both real and imaginary parts) arising from  $\bar{K}K$  related channels, and we shall ignore further renormalization coming from other contributing channels in free space as the  $3\pi$  channel.

To describe the interactions of the  $\phi$  meson with pseudo-scalar mesons and baryons, we follow the model developed in Refs. [13,26]. The Lagrangian describing the coupling of the  $\phi$  meson to kaons reads

$$\mathcal{L}_{\phi,kaons} = -ig_\phi \phi_\mu (K^- \partial^\mu K^+ - K^+ \partial^\mu K^- + \bar{K}^0 \partial^\mu K^0 - K^0 \partial^\mu \bar{K}^0) + g_\phi^2 \phi_\mu \phi^\mu (K^- K^+ + \bar{K}^0 K^0), \quad (1)$$

and it provides, at  $\mathcal{O}(g_\phi^2)$ , a  $\phi$ -meson self-energy  $\Pi_\phi^{free}$  consisting of two-kaon loop contributions and kaon tadpole terms (see Fig. 1). The free width to the  $K\bar{K}$  channel can be

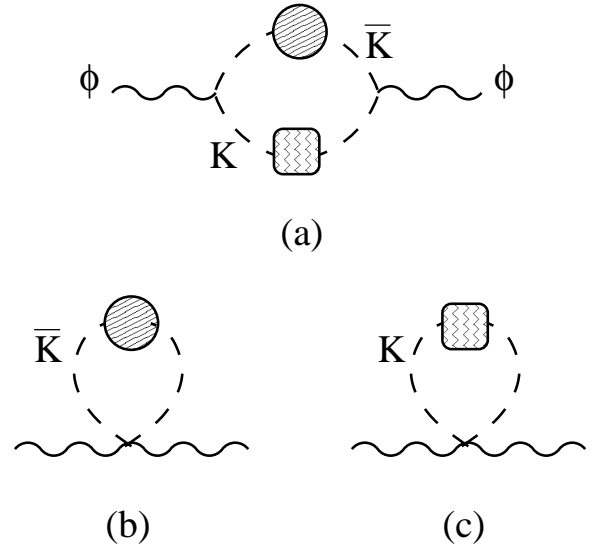


FIG. 2. Medium modified diagrams contributing to the  $\phi$ -meson self-energy in nuclear matter after including kaon self-energies. The dressing of  $\bar{K}(K)$  propagator is indicated by a round (squared) box.

readily calculated from the imaginary part of  $\Pi_\phi^{free}$  and, by comparing to the experimental value of  $\Gamma_{\phi \rightarrow K^+ K^-}$ , one gets  $g_\phi = 4.57$ .

The calculation of the  $\phi$ -meson self-energy in nuclear matter,  $\Pi_\phi^{med}$ , proceeds by a dressing of the kaon propagators including both  $S$ - and  $P$ -wave self-energies, as well as vertex corrections demanded by gauge invariance. We perform a subtraction of the free self-energy  $\Pi_\phi^{free}$  from the in-medium self-energy  $\Pi_\phi^{med}$  which, as we shall discuss below, provides a convergent result. From this in-medium subtracted self-energy,  $\Delta\Pi_\phi^{med} = \Pi_\phi^{med} - \Pi_\phi^{free}$ , the width and mass shift of the  $\phi$  meson will be obtained in Sec. III. Since we are interested in both the real and imaginary parts of the  $\phi$  self-energy, the tadpole terms have to be explicitly included in the calculation and properly modified in the medium. The first step to include the effects of the medium consists of a modification of the kaon propagator with a proper self-energy  $\Pi_K(q^0, \vec{q}; \rho)$ . A diagrammatic representation is shown in Fig. 2.

After this is done, the kaon propagator is given, in its spectral representation [8], by

$$D_{\bar{K}(K)}(q^0, \vec{q}; \rho) = \int_0^\infty d\omega \left( \frac{S_{\bar{K}(K)}(\omega, \vec{q}; \rho)}{q^0 - \omega + i\eta} - \frac{S_{K(\bar{K})}(\omega, \vec{q}; \rho)}{q^0 + \omega - i\eta} \right), \quad (2)$$

where  $S_{\bar{K}(K)}$  is the spectral function of the  $\bar{K}(K)$  meson,

$$S_{\bar{K}(K)}(q^0, \vec{q}; \rho) = -\frac{1}{\pi} \frac{\text{Im}\Pi_{\bar{K}(K)}(q^0, \vec{q}; \rho)}{|(q^0)^2 - \vec{q}^2 - m_K^2 - \Pi_{\bar{K}(K)}(q^0, \vec{q}; \rho)|^2} \quad (3)$$

and  $\Pi_{\bar{K}(K)}$  is the  $\bar{K}(K)$  self-energy in nuclear matter. From now on we take the isospin limit and set  $m_K = m_{\bar{K}} = (m_K +$

$+m_{K^0})/2$ . The in-medium  $\phi$  self-energy arising from dressing the kaon propagators for a  $\phi$  meson at rest reads

$$\begin{aligned} \Pi_{\phi}^{ij}(P^0; \rho) = & \delta^{ij} i 2 g_{\phi}^2 \frac{4}{3} \int \frac{d^4 q}{(2\pi)^4} \vec{q}^2 D_K(P-q; \rho) D_{\bar{K}}(q; \rho) \\ & + \delta^{ij} i 2 g_{\phi}^2 \left\{ \int \frac{d^4 q}{(2\pi)^4} D_{\bar{K}}(q; \rho) \right. \\ & \left. + \int \frac{d^4 q}{(2\pi)^4} D_K(q; \rho) \right\} \equiv \delta^{ij} \Pi_{\phi}(P^0; \rho), \quad (4) \end{aligned}$$

where only spatial components are nonvanishing. If we take a constant self-energy for the kaon, as in Refs. [25,28], the  $dq^0$  and  $d\Omega_q$  integrations can be readily evaluated and the  $\phi$  self-energy takes the simple form

$$\begin{aligned} \Pi_{\phi}(P^0; \rho) = & 2 g_{\phi}^2 \frac{1}{2\pi^2} \frac{4}{3} \int_0^{\infty} dq \vec{q}^2 \left\{ \frac{\vec{q}^2}{\bar{\omega}(q)} \int_0^{\infty} d\omega \right. \\ & \times \frac{S_{\bar{K}}(\omega, |\vec{q}|; \rho) [\omega + \bar{\omega}(q)]}{(P^0)^2 - [\omega + \bar{\omega}(q)]^2 + i\epsilon} \\ & \left. + \frac{3}{4} \left[ \int_0^{\infty} d\omega S_{\bar{K}}(\omega, |\vec{q}|; \rho) + \frac{1}{2\bar{\omega}(q)} \right] \right\}, \quad (5) \end{aligned}$$

where  $\bar{\omega}(q)^2 = \vec{q}^2 + m_K^2 + \Pi_K(\rho)$ .

In the following sections we discuss how the kaon self-energies are obtained. We follow closely Ref. [24] and focus only on the differences introduced in this work.

### A. S-wave kaon self-energy

The interactions of  $K^+$ ,  $K^0$  and  $\bar{K}^0$ ,  $K^-$  with the nucleons of the medium are rather different and it is necessary to treat them separately. Since there are no  $S=1$  baryonic resonances, the  $KN$  interaction is smooth at low energies. We take the approach of Refs. [25,28] where a  $t\rho$  approximation is used and a constant self-energy is obtained.

The  $\bar{K}N$  interaction, however, is dominated at low energies by the excitation of the  $\Lambda(1405)$  resonance, which appears just below the  $\bar{K}N$  threshold. To account for a realistic  $\bar{K}$  self-energy in nuclear matter we follow the coupled channel chiral unitary approach to  $S$ -wave  $\bar{K}N$  scattering developed in Ref. [29]. Starting from this successful scheme in free space, an effective interaction in the medium was obtained in Ref. [25], solving a coupled channel Bethe-Salpeter equation including Pauli blocking on the nucleons, mean-field binding potentials for the baryons involved, and the medium modifications of  $\pi$  mesons and  $\bar{K}$  mesons themselves, leading thus to a self-consistent calculation. By summing over the occupied states in the Fermi sea, the  $\bar{K}$  spectral function was obtained. The inclusion of the  $S$ -wave self-energy accounts for decay channels of the  $\phi$  meson of the type  $KYMh$ , the major contribution coming from  $Y=\Sigma$ ,  $M=\pi$ . The range of validity of this model covers kaon en-

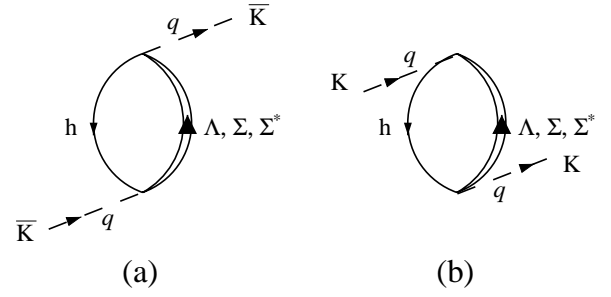


FIG. 3. Kaon  $P$ -wave self-energy diagrams: (a)  $\bar{K}$  direct term; (b)  $K$  crossed term.

ergies and momenta up to 1.5 GeV. Outside this range we take a constant value matching it to the boundary value at energy 1.5 GeV and zero momentum. We have checked that the dependence of our results on the choice of the matching point is negligible. We refer the reader to Refs. [25,29] for details of the model.

### B. P-wave kaon self-energy

Kaons from  $\phi$  decay are emitted with rather low energies, what makes the  $S$ -wave self-energy a major renormalization source to be included in nuclear matter. However, in Refs. [8,24] it was noticed that including  $P$ -wave kaon couplings to nucleons gives rise to a considerable source of renormalization of the  $\phi$  in the medium, leading to a further increase of the  $\phi$  width of the same order as that provided by the  $S$ -wave contribution.

We include  $P$ -wave kaon self-energies accounting for the excitation of  $\Lambda h$ ,  $\Sigma h$ , and  $\Sigma^* h$  pairs [ $\Sigma^* = \Sigma^*(1385)$ ]. The corresponding many-body mechanisms are shown in Fig. 3. Notice that, because of strangeness conservation, only direct terms are permitted for the  $\bar{K}$  excitations. Conversely, the  $K$  self-energy arises from the crossed terms. Since the excited hyperon is far off-shell in the crossed kinematics, we expect the  $K$  to be barely modified by the  $P$ -wave self-energy and we shall not include it in the calculation.

The  $\bar{K}NY$  vertices involved are derived from the lowest order chiral Lagrangian that couples the octet of pseudo-scalar mesons to the  $1/2^+$  baryon octet [25] and then treated in a nonrelativistic approach. The  $P$ -wave  $\bar{K}$  self-energy then reads

$$\begin{aligned} \Pi_{\bar{K}}^{P-wave}(q^0, \vec{q}; \rho) & \equiv \vec{q}^2 \bar{\Pi}_{\bar{K}}^{P-wave}(q^0, \vec{q}; \rho) \\ & = \frac{1}{2} \bar{V}_{K-p\Lambda}^2 f_{\Lambda}^2(q) \vec{q}^2 U_{\Lambda}(q^0, \vec{q}; \rho) \\ & \quad + \frac{3}{2} \bar{V}_{K-p\Sigma}^2 f_{\Sigma}^2(q) \vec{q}^2 U_{\Sigma}(q^0, \vec{q}; \rho) \\ & \quad + \frac{1}{2} \bar{V}_{K-p\Sigma^*}^2 f_{\Sigma^*}^2(q) \vec{q}^2 U_{\Sigma^*}(q^0, \vec{q}; \rho), \quad (6) \end{aligned}$$

where  $U_Y$  ( $Y = \Lambda, \Sigma, \Sigma^*$ ) stands for the Lindhard function

including only direct kinematics, and the  $\tilde{V}_{\bar{K}NY}$  factors contain the required  $\bar{K}NY$  couplings and isospin factors which can be found in Ref. [24].

In the model of Ref. [24] a nonrelativistic treatment of the  $\bar{K}NY$  vertices is used, including relativistic recoil corrections of  $\mathcal{O}(1/M_Y)$ , to deal with the imaginary part of the  $\phi$  self-energy. However, in this work, we are also concerned with the calculation of  $\text{Re}\Pi_\phi^{\text{med}}$  and larger energies and momenta are involved in the loop contributions. We have improved the model of Ref. [24] in the treatment of the relativistic recoil corrections, quoted as the  $f_Y^2(q)$  functions in Eq. (6). Starting from the fully relativistic  $\bar{K}N \rightarrow Y \rightarrow \bar{K}N$  amplitude with an approximately at rest in-medium nucleon and keeping the positive energy intermediate hyperon propagator, we get the following correction factor:

$$f_Y^2(q) = 1 + \frac{(E_Y - M_Y)^2 - (q^0)^2}{4E_Y M_Y}, \quad (7)$$

where  $E_Y = \sqrt{M_Y^2 + \vec{q}^2}$  and  $q^0$  is the kaon energy.

Additionally, to account for the off-shell behavior of the kaon-baryon vertices we have included static dipolar form factors. In Refs. [8,24] relativistic dipolar form factors were used, each  $\bar{K}NY$  vertex carrying a  $[\Lambda^2/(\Lambda^2 - (q^0)^2 + \vec{q}^2)]^2$  factor with  $\Lambda = 1.05$  GeV. In this work, the use of such form factors is not a proper approach because it generates fictitious poles in the loop contributions to the  $\phi$  self-energy. Instead, we choose to use a static version.

To compensate for both changes, we properly rescale the  $\bar{K}NY$  form factors to maintain consistency with the vertices used in Refs. [8,24]. Therefore we multiply each  $\bar{K}NY$  vertex by  $C[\Lambda^2/(\Lambda^2 + \vec{q}^2)]^2$  and we fix the  $C$  constant by performing an on-shell matching to the expressions in Refs. [8,24]. Details on how this matching is done are given in Appendix A.

### C. Vertex corrections and gauge invariance

The introduction of the  $\phi$  coupling to kaons and  $\bar{K}NY$  interactions in a gauge vector description of the  $\phi$  meson generates additional  $\phi\bar{K}NY$  contact interaction vertices. These vertices can be evaluated systematically as done in Ref. [13]. Alternatively, one can also obtain the Feynman rules for these vertices by requiring the  $\phi N \rightarrow KY$  amplitude to vanish when replacing the vector meson polarization by its four-momentum.

At the lowest order in the nuclear density,  $P$ -wave kaon self-energy insertions plus vertex corrections are considered in the diagrams depicted in Fig. 4.

The contribution of diagram (a) in Fig. 4 has already been considered in Eqs. (4) and (5) since it corresponds to a single bubble insertion in the  $\bar{K}$  propagator and it is accounted for by using fully dressed kaon propagators in the calculation of the  $\phi$ -meson self-energy. Diagrams (b)–(d), however, cannot be cast as medium modifications of the meson propagators but as genuine vertex corrections. Let us call  $\Pi_\phi^{\text{VC1}}$  and  $\Pi_\phi^{\text{VC2}}$  the self-energy contributions associated with the sum

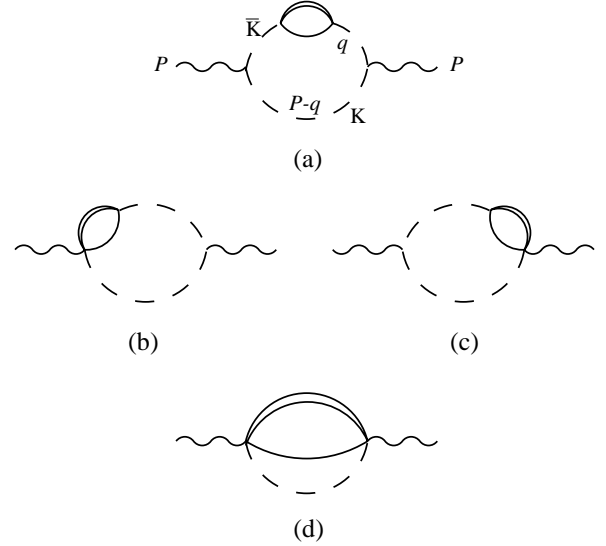


FIG. 4.  $\mathcal{O}(\rho)$  contributions to the  $\phi$  self-energy from  $P$ -wave kaon self-energy insertions and related vertex corrections.

of diagrams (b) and (c) and diagram (d), respectively. Using the Feynman rules derived in Ref. [24] one finds, at first order in density,

$$\begin{aligned} \Pi_\phi^{\text{VC1}}(P^0; \rho) &= i2g_\phi^2 \frac{4}{3} \int \frac{d^4q}{(2\pi)^4} \vec{q}^2 \bar{\Pi}_{\bar{K}}^{P\text{-wave}}(q; \rho) \\ &\quad \times \frac{1}{(P^0 - q^0)^2 - \omega^2(q) + i\epsilon} \frac{1}{(q^0)^2 - \omega^2(q) + i\epsilon}, \end{aligned} \quad (8)$$

$$\begin{aligned} \Pi_\phi^{\text{VC2}}(P^0; \rho) &= i2g_\phi^2 \int \frac{d^4q}{(2\pi)^4} \bar{\Pi}_{\bar{K}}^{P\text{-wave}}(q; \rho) \\ &\quad \times \frac{1}{(P^0 - q^0)^2 - \omega^2(q) + i\epsilon}, \end{aligned} \quad (9)$$

with  $\omega^2(q) = \vec{q}^2 + m_K^2$ . In Eqs. (8) and (9) we have used bare kaon propagators. These results can be further extended to higher orders in density by considering additional self-energy insertions in the kaon propagators. Eventually we substitute the bare kaon propagators in Eqs. (8) and (9) by the fully dressed propagators described in the previous sections. Both contributions  $\Pi_\phi^{\text{VC1}}$ ,  $\Pi_\phi^{\text{VC2}}$  are finite provided that suitable form factors, as discussed in the preceding section, are used in the  $P$ -wave  $\bar{K}NY$  vertices.

In the same line as done for the kaon-nucleon  $P$ -wave interaction, gauge invariance prescribes a coupling of the  $\phi$  meson to the  $S$ -wave  $\bar{K}NMY$  vertices. This coupling is obtained by substituting the ordinary derivative in the meson-baryon chiral Lagrangian of Ref. [29] [see Eq. (5) therein] by a covariant derivative that includes the vector meson field  $SU(3)$  matrix  $V^\mu$  and reads



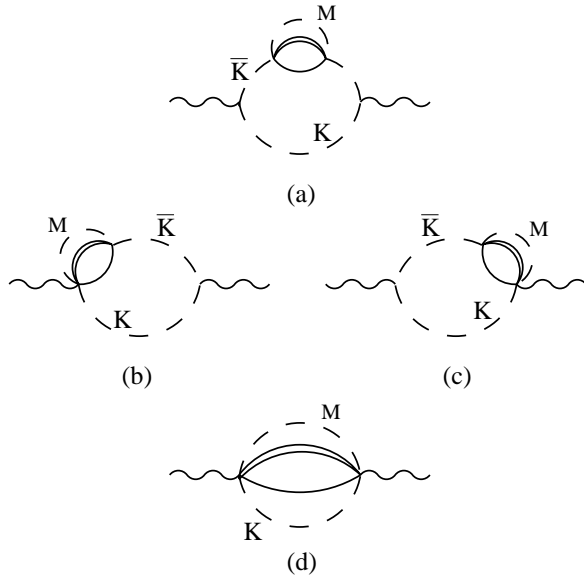


FIG. 5.  $\mathcal{O}(\rho)$  contributions to the  $\phi$  self-energy from  $S$ -wave kaon self-energy insertions and related vertex corrections.

$$\partial^\mu \Phi \rightarrow D^\mu \Phi = \partial^\mu \Phi - i \frac{g}{2} [V^\mu, \Phi], \quad (10)$$

where  $\Phi$  represents the pseudoscalar meson field matrix (we follow the notation of Ref. [13] and therefore  $g_\phi = g/\sqrt{2}$ ). It is also possible to obtain the actual Feynman rules calculating the amplitude  $t_{MY \rightarrow \bar{K}N\phi} \equiv t_{MY \rightarrow \bar{K}N\phi}^\nu \epsilon_\nu(\phi)$ , and requiring  $t_{MY \rightarrow \bar{K}N\phi}^\nu P_\nu = 0$  with  $P$  the four-momentum carried by the  $\phi$ -meson field. The  $\phi$  self-energy diagrams involving  $S$ -wave kaon self-energy insertions plus related vertex corrections are shown in Fig. 5.

As in the case of the  $P$ -wave gauging, the contribution of the first diagram in Fig. 5 is already included in Eqs. (4) and (5) by using the renormalized kaon propagators dressed with the  $S$ -wave self-energy of Ref. [25]. We expect the other three terms [Figs. 5(b)–5(d)] to give a small contribution to the imaginary part of the  $\phi$  self-energy because of the reduced phase space of the intermediate states. We evaluate them in Appendix B and find both the real and imaginary contributions to be negligible as compared to the leading contributions to  $\Pi_\phi^{med}$ .

In addition to the vertex corrections presented in this section one should include also other contributions in which the  $\phi$  meson directly couples to the hyperons. These terms were also considered in Ref. [27] for the case of the  $\rho$  meson self-energy in the medium. We have checked numerically that all of them are about two orders of magnitude smaller than the relevant pieces in the  $\phi$  self-energy, essentially driven by meson self-energy insertions and  $P$ -wave vertex corrections. One of the reasons is that whenever the  $\phi$  is involved in a  $\phi YY$  coupling, there is a hyperon propagator that lies far off-shell in any of these terms.

The introduction of the contact vertices, following a minimal coupling scheme as in Refs. [13,24], guarantees gauge invariance and therefore the  $\phi$  self-energy is transverse. In

our approach, there are small violations of gauge invariance due to the omitted diagrams discussed above, the non-fully-relativistic treatment of the vertices involving baryons, which keep only the lowest orders in a  $(p/M)$  expansion [25]; and also to the fact that only the positive energy part of the hyperon propagators has been included in the calculation. We have explicitly checked that transversality of the  $\phi$  self-energy is achieved at the lowest order in a  $(p/M)$  expansion, where  $p$  is the kaon momentum, when all the diagrams in Figs. 4 and 5, plus those with the  $\phi$  meson coupled to hyperon lines, are considered. In particular, for the  $\phi$  at rest, which is the case under study, this means that  $\Pi_\phi^{00}$ ,  $\Pi_\phi^{i0}$ , and  $\Pi_\phi^{0j}$  vanish at the lowest order that contributes to  $\Pi_\phi^{ij}$  in a  $(p/M)$  expansion. Numerically, we have found that these components are indeed negligible as compared to  $\Pi_\phi^{ij}$ .

We have also checked that, for a  $\phi$  meson at rest, the relevant momenta running in the kaon loops are around 300 MeV. Thus the corrections to the nonrelativistic approximation, which behave as powers of the kaon momentum over the hyperon mass, are expected to be small. However, for high  $\phi$  momenta that are easily obtained in a typical heavy ion collision, a fully relativistic calculation of the interaction vertices and baryon propagators would be advisable.

#### D. Regularization

The  $\phi$ -meson self-energy, as introduced in the previous sections, is a quadratically divergent object either in the medium or in free space, and therefore a regularization procedure is required to remove divergences. Actually, since we are interested in the medium modifications of the  $\phi$  meson, we calculate a subtracted in-medium self-energy,  $\Delta \Pi_\phi^{med}$ , introduced at the beginning of Sec. II. This procedure cancels all divergences leading to a finite result both for the real and imaginary parts of  $\Delta \Pi_\phi^{med}$ . To perform the subtraction we calculate  $\Pi_\phi^{free}$  and  $\Pi_\phi^{med}$  in a momentum cutoff scheme, so that each of them depends on a regularization parameter  $q_{max}$ , but the subtraction gives a finite result in the limit  $q_{max} \rightarrow \infty$ .

Once the vacuum  $\phi$  self-energy is subtracted, one is left, at first order in density, with single meson self-energy insertion diagrams in the propagators and vertex correction involving one baryonic loop. Those diagrams involving  $P$ -wave couplings are convergent once the form factors are considered, as can be seen from power counting. The  $S$ -wave self-energy insertion diagrams are also convergent provided that the high energy-momentum behavior of the  $S$ -wave kaon self-energy is at most a constant, of course density dependent, as in our model.

The convergence of the calculation is easily shown by obtaining explicitly the subtraction of the in-medium  $\phi$  self-energy and the free  $\phi$  self-energy, and using for the  $S$ -wave kaon self-energy its asymptotic value. In a cutoff regularization scheme, the subtraction reads

$$\Pi_{\phi, asympt}^{med} - \Pi_\phi^{free} = C_0 + C_{-2} \frac{1}{q_{max}^2} + \mathcal{O}\left(\frac{1}{q_{max}^3}\right). \quad (11)$$

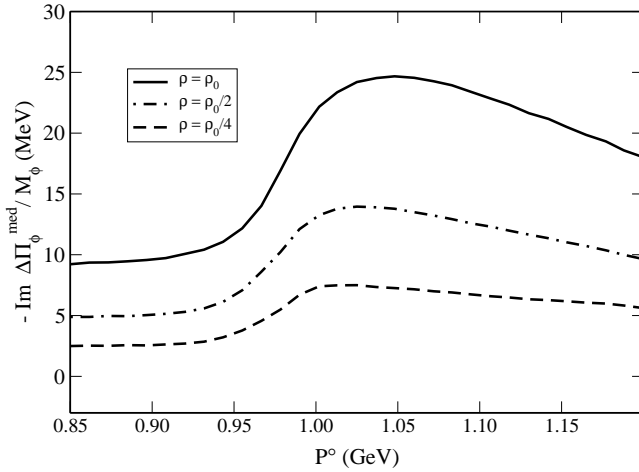


FIG. 6. Imaginary part of the subtracted  $\phi$ -meson self-energy in nuclear matter for several densities.

The quadratic and logarithmic pieces cancel exactly and in the limit  $q_{max} \rightarrow \infty$  we are left with a finite part  $C_0$  that depends on  $P^0$  and the density.

### III. RESULTS AND DISCUSSION

In Fig. 6 we show the imaginary part of the subtracted  $\phi$  self-energy for different densities from  $\rho_0/4$  to  $\rho_0$ . The resulting width of the  $\phi$  meson grows as a function of the density, and after adding the free width it reaches the value of around 30 MeV at the vacuum  $\phi$  mass for normal nuclear density. Most of the  $\phi$  decay channels contributing to the in-medium width have a smooth behavior at the energies under consideration, except for the  $\phi \rightarrow K\Sigma^*h$  channel which, neglecting the  $\Sigma^*$  width, has a threshold at 940 MeV. This threshold moves to higher energies as density grows because of the repulsive potential felt by the kaons. The position of this threshold could be used to constrain the kaon and  $\Sigma^*$  optical potentials.

The results are quite similar in size and shape to those of Ref. [24], except for the more visible bump related to the  $\Sigma^*$  channels. The shape of the imaginary part of the subtracted self-energy also agrees quite well with the results of Ref. [8], although a larger width of around 45 MeV is obtained in that work. The possible reasons of this difference are related to the different approaches in the calculation of the kaon self-energies [24] and the consideration of the recoil factors here.

In Fig. 7, we show the  $\phi$  subtracted width at normal nuclear density obtained by successively considering different choices of antikaon self-energy and the inclusion of vertex corrections. In all cases we use the full  $S$ -wave repulsive kaon self-energy in the calculation. The lowest curve corresponds to the  $\phi$  subtracted medium width when the  $\bar{K}$  propagator incorporates only the  $S$ -wave  $\bar{K}$  self-energy. This self-energy is mildly attractive, compensating in part the repulsion felt by the kaon. Its imaginary part comes from the kaon decaying into  $\pi\Lambda h$  and  $\pi\Sigma h$  and therefore this corresponds to the  $\phi$  decay channels  $\phi \rightarrow K\pi\Lambda h$  and  $\phi \rightarrow K\pi\Sigma h$ .

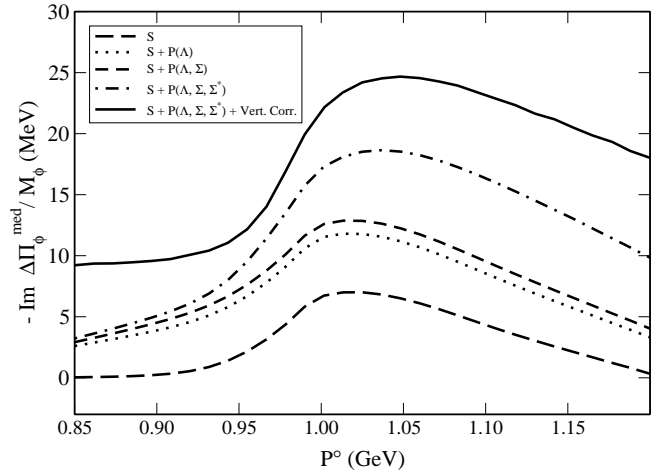


FIG. 7. Contributions to the imaginary part of the subtracted  $\phi$ -meson self-energy in nuclear matter at  $\rho = \rho_0$ .

In the next curves, we consider additionally the  $P$ -wave  $\bar{K}$  self-energy due to the kaon coupling to  $\Lambda h$ ,  $\Lambda h + \Sigma h$ , and  $\Lambda h + \Sigma h + \Sigma^* h$  excitations. We find a quite small contribution from the  $\Sigma$  and sizable contributions from the  $\phi N \rightarrow K\Lambda$  and  $\phi N \rightarrow K\Sigma^*$  processes. As commented above, the  $\Sigma^*$  channel has its threshold around 940 MeV and therefore only contributes strongly above this energy. The small contribution below the threshold, visible in the figure, is due to the approximation of using a constant  $\Sigma^*$  width in the calculation. The  $\phi N \rightarrow K\Lambda$  channel has a much lower threshold and thus its contribution depends little on energy. Finally, the solid line also incorporates the vertex corrections leading to a further enhancement of the total width.

In Fig. 8 we show the real part of  $\Delta\Pi_\phi^{med}$  which we find mildly attractive up to energies around 1.1 GeV. The change in the  $\phi$  mass at  $\sqrt{s} = M_\phi$  is approximately 8 MeV to lower energies at  $\rho = \rho_0$ . This small correction is in agreement with previous works [8,10], although it disagrees with naive scaling expectations. There are recent experimental results at  $T = 0$  [30] which do not observe any signature of in-medium

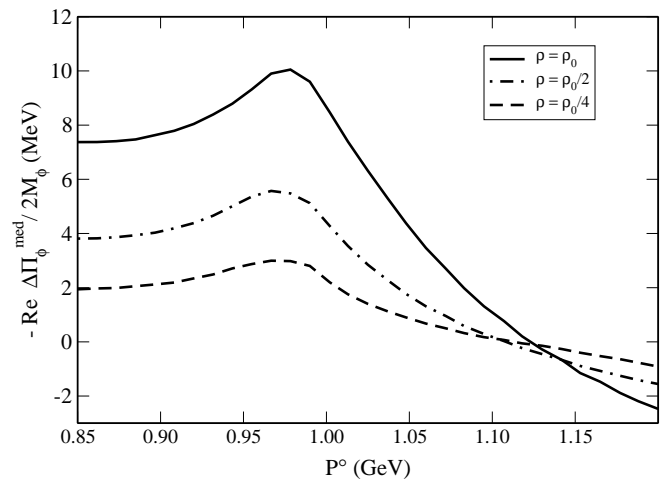


FIG. 8. Real part of the subtracted  $\phi$ -meson self-energy in nuclear matter for several densities.

modification of the  $\phi$  mass in the reaction  $pA \rightarrow K^+ K^- X$ . However, one should be careful in the interpretation of the results without a detailed theoretical calculation. On the one hand, the distortion of the final kaons and the initial protons could force the reaction to occur at the nuclear surface and therefore at low densities. On the other hand, due to the long  $\phi$  lifetime and the large average  $\phi$  momentum a good part of the events could correspond to  $\phi$  decays in vacuum. Furthermore, for those events with a fast  $\phi$  meson, the use of a self-energy obtained for a  $\phi$  at rest is not justified.

In summary, we have studied the  $\phi$  self-energy for a  $\phi$  at rest in a cold, symmetric nuclear medium, by considering the medium effects over the tadpole and  $K\bar{K}$  decay diagrams which dominate the  $\phi$  vacuum self-energy. This has been done by dressing the kaons with  $S$ - and  $P$ -wave self-energies. The  $S$ -wave antikaon self-energy was obtained in a self-consistent coupled channel unitary calculation based on effective chiral Lagrangians in which Pauli blocking, pion self-energy, and mean-field potentials of the baryons are taken into account. The  $P$  wave is driven by the coupling to hyperon-hole excitations. In addition to these self-energy insertions we have calculated a set of vertex corrections required by gauge invariance. We obtain a small mass shift of around 8 MeV and a width of around 30 MeV at normal nuclear density. Thus, the main medium effect on the  $\phi$  meson is the growth of its width by almost one order of magnitude at normal nuclear density. Nevertheless, the  $\phi$  stays narrow enough to be visible as an isolated resonance and then give a clear signal in possible experiments measuring dilepton or  $\bar{K}K$  spectra.

#### ACKNOWLEDGMENTS

We thank E. Oset for fruitful discussions. We acknowledge partial financial support from the DGICYT under Contract No. BFM2000-1326. D.C. thanks MCYT for financial support.

#### APPENDIX A: ON-SHELL MATCHING OF $\bar{K}NY$ STATIC FORM FACTOR

In this work we have used the model of Ref. [24] for the  $\bar{K}$  self-energy. However, as we are interested in the real part of the  $\phi$  self-energy and therefore need to evaluate loop contributions, we have introduced new  $\bar{K}NY$  form factors and more precise recoil corrections. In order to maintain consistency with the coupling of previous calculations [8,24] we match our couplings at the appropriate kinematic conditions. Let us consider the process depicted in Fig. 9 in which a  $\phi$  meson decays into a kaon and  $Yh$  excitation.

It corresponds to the unitary cut of the self-energy diagram in Fig. 4(a) and relates to the  $\phi$ -nucleon scattering process  $\phi N \rightarrow KY$ . In the situation of a  $\phi$  at rest with respect to the nuclear medium the energies and momenta carried by the on-shell  $K$  and the off-shell  $\bar{K}$  are given by

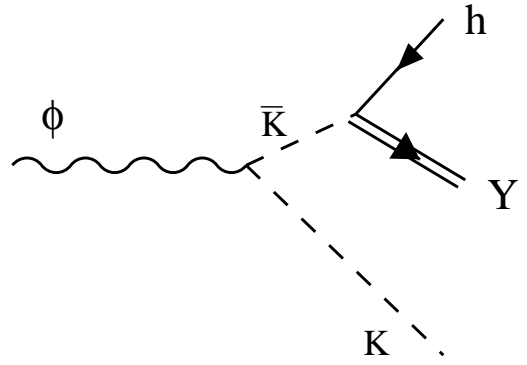


FIG. 9.  $\phi$  meson decay into a  $K$  meson and a  $Yh$  excitation.

$$E_K = \frac{(M_N + M_\phi)^2 + m_K^2 - M_Y^2}{2(M_N + M_\phi)},$$

$$E_{\bar{K}} = M_\phi - E_K,$$

$$|\vec{q}|_K = |\vec{q}|_{\bar{K}} = \sqrt{E_K^2 - m_K^2}. \quad (\text{A1})$$

The matching proceeds by demanding the following equality to be satisfied:

$$\begin{aligned} C^2 \left( \frac{\Lambda^2}{\Lambda^2 + |\vec{q}|_K^2} \right)^4 f_Y^2(E_{\bar{K}}, |\vec{q}|_{\bar{K}}) \\ = \left( \frac{\Lambda^2}{\Lambda^2 - E_{\bar{K}}^2 + |\vec{q}|_K^2} \right)^4 f_{0Y}^2(E_{\bar{K}}), \end{aligned} \quad (\text{A2})$$

what fixes the value of the scaling constant  $C$  in terms of the chosen cutoff parameter  $\Lambda = 1.05$  GeV [8,24]. We set  $M_Y$  to an average value of 1200 MeV,  $f_Y^2$  is given in Eq. (7), and  $f_{0Y}^2 = [1 - E_{\bar{K}}/(2M_Y)]^2$  is the recoil factor of Ref. [24]. We get a scaling constant value of  $C = 1.04$ .

#### APPENDIX B: S-WAVE GAUGING TERMS

We evaluate here the self-energy contributions from diagrams in Figs. 5(b)–5(d). The necessary Feynman rules for the vertices involved (Fig. 10) are given by

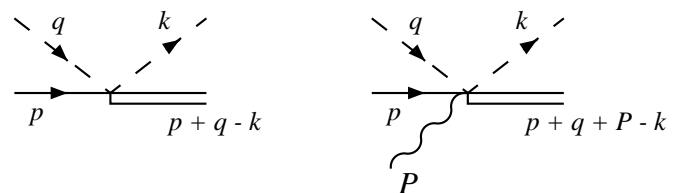


FIG. 10.  $S$ -wave kaon-nucleon vertex and the corresponding  $\phi$  contact coupling.

$$\begin{aligned}
-it_{\bar{K}NMY} &= i \frac{1}{4f^2} C_{i,f} \gamma^\mu (q+k)_\mu \\
-it_{\bar{K}NMY\phi} &= ig_\phi \frac{1}{4f^2} C_{i,f} \gamma^\mu \epsilon_\mu(\phi), \quad (\text{B1})
\end{aligned}$$

where the  $C_{i,f}$  coefficients, related to the initial and final states, can be found in Ref. [29]. We use a nonrelativistic reduction of these vertices which is enough to determine the size of the imaginary part. We only keep the temporal components in the slash appearing in  $t_{\bar{K}NMY}$  and the  $\mathcal{O}(1/M_B)$  terms in  $t_{\bar{K}NMY\phi}$ . In addition, we neglect terms linear in the hole momentum. We select the case of an intermediate  $\pi^0\Lambda$  state, which is the one less disfavored in phase space. Under these assumptions we find

$$\begin{aligned}
\Pi_\phi^{VC1'}(P^0; \rho) &= -ig_\phi^2 \frac{1}{128f^4 M_\Lambda \pi^2} \frac{1}{P^0} \left\{ \mathcal{P} \int_0^\infty dq \frac{\vec{q}^2}{\omega_K(q)} \right. \\
&\times \left[ \frac{I[-P^0 - \omega_K(q), |\vec{q}|]}{P^0 + 2\omega_K(q)} + \frac{I[-\omega_K(q), |\vec{q}|]}{P^0 - 2\omega_K(q)} \right] \\
&\left. - i\pi \frac{|\vec{q}_{on}|}{2} I(-P^0/2, |\vec{q}_{on}|) \theta(P^0 - 2m_K) \right\}, \quad (\text{B2})
\end{aligned}$$

with  $I(q^0, |\vec{q}|) = -i/(2\pi)^2 \int_0^\infty dk \vec{k}^2 [q^0 + P^0 - \omega_\pi(k)] / 2\omega_\pi(k) \int_{-1}^1 du (\vec{q}^2 - \vec{q} \cdot \vec{k}) U_\Lambda[q^0 + P^0 + \omega_\pi(k), \vec{q} - \vec{k}; \rho/2]$ ,

$\sigma(P^0) = \sqrt{1 - 4m_K^2/(P^0)^2}$ ,  $|\vec{q}_{on}| = \sigma(P^0) P^0/2$ ,  $\omega_K(q) = \sqrt{\vec{q}^2 + m_K^2}$ ,  $\omega_\pi(k) = \sqrt{\vec{k}^2 + m_\pi^2}$ , and  $u \equiv \vec{q} \cdot \vec{k} / |\vec{q}| \cdot |\vec{k}|$  for diagrams (b) and (c), and

$$\begin{aligned}
\Pi_\phi^{VC2'}(P^0; \rho) &= ig_\phi^2 \frac{3}{256f^4 M_\Lambda^2} \frac{1}{2\pi^2} \\
&\times \int_0^\infty dq \frac{\vec{q}^2}{2\omega_K(q)} \tilde{I}[-\omega_K(q), |\vec{q}|], \quad (\text{B3})
\end{aligned}$$

with

$$\begin{aligned}
\tilde{I}(q^0, |\vec{q}|) &= \frac{-i}{(2\pi)^2} \int_0^\infty dk \frac{\vec{k}^2}{2\omega_\pi(k)} \int_{-1}^{+1} du (\vec{q} - \vec{k})^2 \\
&\times U_\Lambda[q^0 + P^0 + \omega_\pi(k), \vec{q} - \vec{k}; \rho/2]
\end{aligned}$$

for diagram (d). The imaginary parts of  $\Pi_\phi^{VC1'}$  and  $\Pi_\phi^{VC2'}$  are finite and very small compared to the contributions of meson self-energy insertions and  $P$ -wave vertex corrections. The real parts are divergent and one has to regularize both the  $\pi$ - $Yh$  loop and the external kaon loop. Under reasonable momentum cutoffs (1–2 GeV) we find that the real parts are of the same order as the imaginary parts and thus negligible compared to the leading contributions.

- 
- [1] R. Rapp and J. Wambach, *Adv. Nucl. Phys.* **25**, 1 (2000).  
[2] C.J. Batty, E. Friedman, and A. Gal, *Phys. Rep.* **287**, 385 (1997).  
[3] S. Hirenzaki, Y. Okumura, H. Toki, E. Oset, and A. Ramos, *Phys. Rev. C* **61**, 055205 (2000).  
[4] A. Baca, C. Garcia-Recio, and J. Nieves, *Nucl. Phys.* **A673**, 335 (2000).  
[5] A. Gal, *Nucl. Phys.* **A691**, 268 (2001).  
[6] D.B. Kaplan and A.E. Nelson, *Phys. Lett. B* **175**, 57 (1986).  
[7] S. Pal, C.M. Ko, and Z.w. Lin, *Nucl. Phys.* **A707**, 525 (2002).  
[8] F. Klingl, T. Waas, and W. Weise, *Phys. Lett. B* **431**, 254 (1998).  
[9] E. Oset, M.J. Vicente Vacas, H. Toki, and A. Ramos, *Phys. Lett. B* **508**, 237 (2001).  
[10] H. Kuwabara and T. Hatsuda, *Prog. Theor. Phys.* **94**, 1163 (1995).  
[11] C. Song, *Phys. Lett. B* **388**, 141 (1996).  
[12] A. Bhattacharyya, S.K. Ghosh, S.C. Phatak, and S. Raha, *Phys. Rev. C* **55**, 1463 (1997).  
[13] F. Klingl, N. Kaiser, and W. Weise, *Nucl. Phys.* **A624**, 527 (1997).  
[14] M. Asakawa and C.M. Ko, *Nucl. Phys.* **A572**, 732 (1994).  
[15] S. Zschocke, O.P. Pavlenko, and B. Kampfer, *nucl-th/0205057*.  
[16] J.P. Blaizot and R. Mendez Galain, *Phys. Lett. B* **271**, 32 (1991).  
[17] C.M. Ko, P. Levai, X.J. Qiu, and C.T. Li, *Phys. Rev. C* **45**, 1400 (1992).  
[18] E.V. Shuryak and V. Thorsson, *Nucl. Phys.* **A536**, 1400 (1992).  
[19] D. Lissauer and E.V. Shuryak, *Phys. Lett. B* **253**, 15 (1991).  
[20] A.R. Panda and K.C. Roy, *Mod. Phys. Lett. A* **8**, 2851 (1993).  
[21] C.M. Ko and D. Seibert, *Phys. Rev. C* **49**, 2198 (1994).  
[22] W. Smith and K.L. Haglin, *Phys. Rev. C* **57**, 1449 (1998).  
[23] L. Alvarez-Ruso and V. Koch, *Phys. Rev. C* **65**, 054901 (2002).  
[24] E. Oset and A. Ramos, *Nucl. Phys.* **A679**, 616 (2001).  
[25] A. Ramos and E. Oset, *Nucl. Phys.* **A671**, 481 (2000).  
[26] F. Klingl, N. Kaiser, and W. Weise, *Z. Phys. A* **356**, 193 (1996).  
[27] D. Cabrera, E. Oset, and M.J. Vicente Vacas, *Nucl. Phys.* **A705**, 90 (2002).  
[28] N. Kaiser, P.B. Siegel, and W. Weise, *Nucl. Phys.* **A594**, 325 (1995).  
[29] E. Oset and A. Ramos, *Nucl. Phys.* **A635**, 99 (1998).  
[30] K. Ozawa *et al.*, *Nucl. Phys.* **A698**, 535 (2002).